Decomposing the dynamics of the Lorenz 1963 model using unstable periodic orbits: Averages, transitions, and quasi-invariant sets

Cite as: Chaos **32**, 033129 (2022); https://doi.org/10.1063/5.0067673
Submitted: 18 August 2021 • Accepted: 21 February 2022 • Published Online: 23 March 2022

Chiara Cecilia Maiocchi, Valerio Lucarini and Andrey Gritsun

Decomposing the dynamics of the Lorenz 1963 model using unstable periodic orbits: Averages, transitions, and quasi-invariant sets

Cite as: Chaos **32**, 033129 (2022); doi: 10.1063/5.0067673
Submitted: 18 August 2021 · Accepted: 21 February 2022 ·
Published Online: 23 March 2022

Chiara Cecilia Maiocchi,[1,2,a)] Valerio Lucarini,[1,2,b)] and Andrey Gritsun[3,c)]

AFFILIATIONS

[1]Centre for the Mathematics of Planet Earth, University of Reading, Reading RG6 6AH, United Kingdom
[2]Department of Mathematics and Statistics, University of Reading, Reading RG6 6AH, United Kingdom
[3]Institute of Numerical Mathematics, Russian Academy of Sciences, Moscow 119333, Russia

Note: This article is part of the Focus Issue, Theory-informed and Data-driven Approaches to Advance Climate Sciences.
[a)]**Author to whom correspondence should be addressed:** c.maiocchi@pgr.reading.ac.uk
[b)]**Email:** v.lucarini@reading.ac.uk
[c)]**Email:** asgrit@mail.ru

ABSTRACT

Unstable periodic orbits (UPOs) are a valuable tool for studying chaotic dynamical systems, as they allow one to distill their dynamical structure. We consider here the Lorenz 1963 model with the classic parameters' value. We investigate how a chaotic trajectory can be approximated using a complete set of UPOs up to symbolic dynamics' period 14. At each instant, we rank the UPOs according to their proximity to the position of the orbit in the phase space. We study this process from two different perspectives. First, we find that longer period UPOs overwhelmingly provide the best local approximation to the trajectory. Second, we construct a finite-state Markov chain by studying the scattering of the orbit between the neighborhood of the various UPOs. Each UPO and its neighborhood are taken as a possible state of the system. Through the analysis of the subdominant eigenvectors of the corresponding stochastic matrix, we provide a different interpretation of the mixing processes occurring in the system by taking advantage of the concept of quasi-invariant sets.

The attractor of a chaotic system is densely populated by an infinite number of unstable periodic orbits (UPOs), which are exact periodic solutions of the evolution equations. UPOs can be used to decompose the complex phenomenology of a chaotic flow into elementary components and have shown great potential for the understanding of macroscopic features in turbulent fluid flows. Here, we investigate how a long forward trajectory of the celebrated Lorenz 1963 model featuring the classical parameters' value can be seen as a scattering process where the scatterers are the UPOs. This process helps elucidate how a generic ensemble of initial conditions converges to the invariant measure through diffusion and provides a new interpretation of quasi-invariant sets of the system in terms of UPOs.

I. INTRODUCTION

Unstable periodic orbits (UPOs) play an important role in the analysis of dynamical systems that exhibit chaotic behavior. As noticed early on by Poincaré,[1] UPOs provide a powerful framework for understanding their statistical properties[2] (see ChaosBook[3] for an extensive discussion of this). UPOs can be considered as islets of order in a landscape of chaos and can be used to reconstruct the statistical properties of a chaotic dynamical system.[4] In fact, when UPOs are dense in the attractor,[5] they can approximate with an arbitrary accuracy any trajectory in the system on the attractor.[6] This is possible because the trajectory is continuously repelled from the neighborhood of one UPO to another, as a result of the instability of the UPOs. Within this context, it is possible to develop a theory that

allows dynamical averages to be written as weighted sums over the full set of UPOs. Gutzwiller[7] first demonstrated that UPOs are the essential building blocks of chaotic dynamics. Cvitanović[8] argued that UPOs are the optimal practical tool for measuring the invariant properties of a dynamical system. Ruelle, in turn, derived the dynamical ζ function,[9] which allows one to write averages over the invariant measure of the system as a weighted sum over the infinite set of UPOs.

These results are proven to be valid for a special set of dynamical systems exhibiting strong chaoticity,[10,11] such as uniformly hyperbolic and Axiom A systems.[12,13] However, in complex models of fluid flows, it is often difficult, if not impossible, to verify the hypothesis required for the validity of periodic orbit expansion. When turbulent conditions are considered, such systems live, after transients have died out, in nonequilibrium steady state (NESS).[14] This state is, in general, characterized by the generation of entropy, contraction of phase space, and finite-time predictability. The "*chaotic hypothesis*" of Gallavotti offers a possible solution to the first problem, allowing to consider "*a turbulent fluid as a transitive Axiom A system for the purpose of computing macroscopic properties of the system*."[15,16]

It is usually assumed that considering short-period UPOs allows for a sufficiently accurate estimate of ergodic averages.[17–19] Indeed, some authors have attempted to define what is the optimal choice of low-period UPOs for approximating ergodic averages of given observables for both discrete[20] and continuous-time[21] dynamical systems. Note that, instead, Zoldi and Greenside[22] have emphasized that in some cases long-period UPOs are essential for achieving good accuracy when performing averages. Along these lines, Lasagna[23,24] found numerical evidence that long-period UPOs could be used as accurate proxies of chaotic trajectories. His proposal, in contrast with the previous authors, is that few long UPOs might be able to capture the statistical properties of chaotic trajectories. One should keep in mind that the efficient computation of UPOs in high-dimensional systems still represents an open challenge.[25]

A. Unstable periodic orbits: Applications

The first application of periodic orbit expansion was performed by Auerbach *et al.*,[26] where they proved that UPOs are experimentally accessible and capable of unfolding the structure of chaotic trajectories. In fact, by extracting the complete set of UPOs of symbolic length up to period n and calculating their instability, they approximated the fractal dimension and topological entropy of the strange attractor of the paradigmatic Hénon map with very high accuracy. Artuso *et al.* tested this procedure through a series of applications[19,27] and demonstrated that the cycle expansion of the dynamical ζ function is instrumental for the analysis of deterministic chaos, even in more generic settings than the ones required by Ref. 8, i.e., when the system is not uniformly hyperbolic. Eckhardt and Ott[17] presented one of the first numerical applications of the periodic orbit formalism for studying the statistical and the dynamical properties of the Lorenz 1963 (L63) system.[28] A subsequent analysis of the linear and nonlinear response of the L63 to perturbations shows that specific UPOs are responsible for resonance mechanisms leading to an amplified response.[29]

Later on, periodic orbit theory found fruitful applications also within the context of higher dimensional NESSs, and specifically in the case of (geophysical) fluid dynamics. Even though a complete UPOs-based analysis of turbulent flows is still a far reaching goal, many steps have been made in this direction.[30] Kawahara and Kida,[31] who found a UPO embedded in the attractor of a numerical simulation of plane Couette flow, showed that one UPO only manages to capture in a surprisingly accurate way the turbulence statistics. At a moderate Reynolds number, Chandler and Kerswell[25] identified 50 UPOs of a turbulent fluid and used them to reproduce the energy and dissipation probability density functions of the system as dynamical averages over the orbit. These encouraging results suggested that periodic orbit theory could represent a valid investigation tool also in the realm of climate systems.

In the geophysical context, Gritsun[32,33] proposed the use of an expansion over UPOs to reconstruct the statistics of a simple atmospheric model based on the barotropic vorticity equation of the sphere. Gritsun and Lucarini[34] used the UPOs for interpreting nontrivial resonant responses to force that underlined the violation of the standard fluctuation–dissipation relation for NESS for deterministic chaotic systems. Lucarini and Gritsun[35] used UPOs for clarifying the nature of blocking events in a baroclinic model of the atmosphere. Specifically, they found that blocked states are associated with conditions of higher instability of the atmosphere, in agreement with a separate line of evidence.[36] Additionally, the analysis of UPOs was instrumental in proving that the atmospheric model was characterized by variability in the number of unstable dimensions, which implies a very strong violation of hyperbolicity.[37]

The analysis by Lucarini and Gristun[35] proposed the idea that the observed blocked states of the atmospheric flow should be interpreted as conditions where there is not only proximity of the trajectory to special classes of UPOs but also co-evolution, at least locally in time (the so-called *shadowing*). This implies that blocking can be associated with actual nonlinear modes of the atmosphere.

This calls for looking at both the proximity and the co-evolution of chaotic trajectories with approximating UPOs. Recent investigations have been carried out exactly in this direction, yet in a different context. Both Yalnız and Budanur[38] and Krygier *et al.*[39] investigated the process of shadowing of time-periodic solutions in three-dimensional fluids, although using different shadowing metrics, providing numerical evidence of the shadowing of a trajectory in terms of UPOs. In particular, in Ref. 38, the authors explored a topological approach that makes use of persistence analysis to quantify the shape similarity of chaotic trajectory segments and periodic orbits. In Ref. 39, the authors investigated whether three-dimensional turbulent flows shadow time-periodic solutions. It is worth noticing that both studies investigate the properties of non-hyperbolic chaotic systems, whereas the Lorenz system is almost-everywhere uniformly hyperbolic.

B. This paper

This paper aims at contributing to the understanding of how UPOs can be used for distilling the dynamical and statistical properties of chaotic systems. We consider the L63 model as a test case. The use of UPOs for performing accurate estimates of statistical averaging of test observables has already been extensively debated

in the literature (see discussion in Sec. II B). We will not delve into this matter, but we rather focus on shedding light on the shadowing process. In particular, at each point in time, we rank in different tiers the UPOs of our database based on their distance with respect to the trajectory (the first tier containing the closest orbits, the *Kth* tier containing the K closest orbits, etc.) and we study the persistence of the ranking. Our goal is twofold. On the one hand, we aim to numerically understand how chaotic trajectories are approximated in terms of UPOs. We anticipate that it emerges that longer period UPOs play a major role in reproducing the invariant measure of the system. On the other hand, we study the statistics of the scattering of the orbit between the various UPOs.

This study of scattering uses a partition of the phase space of the L63 model that is different than the classical Ulam's partition.[40] Each UPO (and its immediate neighborhood) is interpreted as a building block of the system, a spatially extended state, and the scattering can be seen as subsequent transitions between different states; see also the recent study of a turbulent flow performed along these lines.[41]

We will show that this viewpoint allows for a different interpretations of quasi-invariant sets.[42] In particular, by studying the spectral properties of the discretized transfer operator, we obtain a partition of the phase space in different bundles of UPOs, each one identifying a quasi-invariant region. We prove that UPOs represent a valid tool to investigate diffusion properties of the system, in fact, being exact solutions, they retain a memory of the geometrical structure of the attractor.

The structure of the rest of the paper is as follows. In Sec. II, we present the UPOs database we consider and describe our analysis of the shadowing and discuss its statistical properties. We prove the robustness of the results independent of the shadowing criteria. In Sec. III, we construct the discretized transfer operator in terms of a finite-state stochastic matrix and use it to describe the scattering of the chaotic trajectory by the various UPOs. We identify quasi-invariant sets through the study of the spectrum of the transition matrix and investigate the decay of correlations associated with the relaxation process of the arbitrary ensemble to the invariant measure. In Sec. IV, we outline our conclusions and perspectives for future works. In Appendix A, we provide a more extensive description of the algorithms considered for our analysis, and in Appendix B, we briefly recapitulate some of the main properties of quasi-invariant sets. The supporting data[43] provides the raw data produced in the course of this work, extra figures, videos, and further details on the methodology.

II. SHADOWING OF THE MODEL TRAJECTORY BY UNSTABLE PERIODIC ORBITS

A. Mathematical framework

We consider a continuous-time autonomous dynamical system $\dot{x} = f(x)$ on a compact manifold $\mathcal{M} \subset \mathbb{R}^n$. We have that $x(t) = S^t x_0$, where $x_0 = x(0)$ is the initial condition and S^t is the evolution operator defined for $t \in \mathbb{R}_{t>0}$. We assume that the system is dissipative ($\nabla \cdot f < 0$). We define $\Omega \subset M$ as the compact attracting invariant set of the dynamical system that supports a unique invariant physical measure ρ. Hence, for any sufficiently regular function (observable) $\varphi : M \to \mathbb{R}$, we have that

$$\langle \varphi \rangle = \int \rho(dx)\varphi(x) = \lim_{T\to\infty} \frac{1}{T} \int_0^T \varphi(S^t x_0)\, dt \tag{1}$$

for almost all initial conditions x_0 belonging to the basin of attraction of Ω. Another key concept we already mentioned is the one of the periodic orbits. A periodic orbit of period T is defined as

$$S^T(x) = x. \tag{2}$$

This representation is not unique. In fact, if Eq. (2) is satisfied, $S^{nT}(x) = x$ is verified as well $\forall n \in \mathbb{N}$. By the semigroup property of the evolution operator, we also have that $S^T(y) = y$ if $y = S^s(x)$ for any choice of s. From now onward, we will consider a periodic orbit to be identified by its prime period $T > 0$ (we do not consider equilibria) and an initial condition x_0.

We consider here *chaotic* dynamical systems. By chaotic, we indicate the property of sensitive dependence on initial conditions on the attractor. In particular, the first Lyapunov exponent Λ_1, which gives information on the average asymptotic rate of divergence of initially infinitesimally nearby trajectories, is positive.[44]

As discussed above, the attractor of a chaotic system is densely populated by UPOs, which provide key information on the system despite being non-chaotic themselves. Indeed, a forward trajectory on the attractor can alternatively be seen as undergoing a process of scattering between the neighborhood of the various UPOs. For a while, the trajectory shadows—see later discussion—a nearby UPO before being repelled. The UPOs act as scattering centers exactly as a result of their instability. Additionally, the invariant measure can be reconstructed through the use of trace formulas[3] by considering the following expression for the average of any measurable observable φ:

$$\langle \varphi \rangle = \lim_{t\to\infty} \frac{\sum_{UP, p\le t} w^{UP} \bar{\varphi}^{UP}}{\sum_{UP, p\le t} w^{UP}}, \tag{3}$$

where U^p is a UPO of prime period p, w^{UP} is its weight, and $\bar{\varphi}^{UP}$ is the average in time of the observable along the orbit. For uniformly hyperbolic dynamical systems, this result is exact and the weight can be obtained, to a first approximation, by $w^{UP} \propto \exp(-p h_{ks}^{UP})$,[4] with h_{ks} being the Kolmogorov–Sinai entropy of the system. This quantity provides information on the rate of creation of information due to the chaoticity of the system. From the knowledge of the spectrum of Lyapunov exponents of the system Λ_i, $i = 1, \ldots, n$,[44] we can find an explicit expression for h_{ks} via the Pesin theorem,[45]

$$h_{ks} \le \sum_{\Lambda_i > 0} \Lambda_i, \tag{4}$$

where the left and right hand sides are equal if the invariant measure is of the Sinai–Ruelle–Bown (SRB) type.[5]

B. The model

Our analysis is performed on the L63 model, which arguably is the most paradigmatic continuous-time chaotic system. The evolution equations of the L63 model are

$$\dot{x} = \sigma y - \sigma x,$$
$$\dot{y} = Rx - y - zx,$$
$$\dot{z} = -\beta z + xy,$$

where the three parameters σ, R, and β are positive numbers, descriptive of the Prandtl number, of the Rayleigh number, and of the geometry of the system. For specific choices of the parameters' value, the attractor is a strange set and the dynamics is characterized by sensitive dependence on initial conditions.[46] Additionally, the attractor is densely populated by an infinite number of UPOs.[47]

In this work, we consider the standard parameters value $\sigma = 10$, $R = 28$, and $\beta = 8/3$. For such values, the dynamics of the system is characterized by a chaotic behavior on a singularly hyperbolic attractor that supports an SRB measure.[48]

Many studies on UPOs of the Lorenz system have been carried out. Eckhardt and Ott[17] presented one of the first numerical applications of the periodic orbit formalism by considering an approximate symbolic coding[8] (UPOs with a period up to 9) to calculate Hausdorff dimensions and Lyapunov exponents. Franceschini *et al.*[49] calculated a number of UPOs of the Lorenz attractor at both standard and nonstandard parameter values and used them to approximate the topological entropy and Hausdorff dimension. Zoldi[50] investigated to what extent trace formulas can predict the structure of the histogram of chaotic time series data extracted from the run of the L63 model with different parameter values. The use of a correct weighting in the trace formula has been extensively investigated.[51–53]

C. The database

Many numerical algorithms have been proposed so far. Saiki[54] reviewed the Newton–Raphson–Mees method, proposing a value for the damping coefficient related to the stability exponent of the orbit, while Barrio *et al.*[55] carried out an extensive high-precision numerical simulation in order to gather a benchmark database of UPOs for L63. It is possible to construct a symbolic dynamics that characterizes uniquely the UPOs of the L63 model.[56] Motivated by the work of Galias and Tucker,[57] who computed all $M = 2536$ UPOs of symbolic sequence period up to 14, we use this set of UPOs for the rest of our analysis. The UPOs are computed using Newton's method (see Appendix A for more details). The statistics of prime periods is shown in Fig. 1. The periods span from $T_{min} = 1.5587$ to $T_{max} = 10.8701$, and our sample presents the characteristic exponential growth with the period.[58] The values of Λ_1 range from 0.756 to 0.994 and agree within an error of 1% with the values of Λ_1 obtained in Ref. 56. No UPO has a vanishing or negative value of Λ_1 (which would go against the chaotic nature of the flow).

Note that, as is well known, the local instability of the L63 model varies wildly within its attractor, where regions with very high instability alternate with regions where one observes return-of-skill for finite-time forecast.[59] Hence, in this case, as opposed to what observed in Ref. 35, the heterogeneity of the attractor in terms of instability cannot be explained using the properties of the individual UPOs, possibly because we are considering here a very low-dimensional flow, whereas a higher level of detail at the spatial level would be needed.

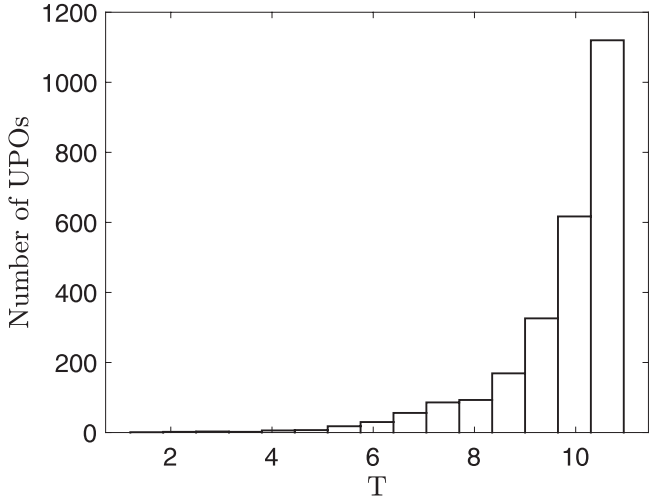

FIG. 1. Number of UPOs in our database vs their prime period. We have considered symbolic sequences of a period up to 14.

D. Ranked shadowing of the chaotic trajectory

We present here our results on how the UPOs rank shadow a long chaotic trajectory. The data reported below refer to a chaotic trajectory $\mathscr{X}_{chaotic}$ of duration $T_{max} = 10^5$, where the output is given every $dt = 0.01$. This leads to considering the set of points $\mathscr{X}_{chaotic} = \{x_t\}_{t=1}^{N_{max}}$, where N_{max} is $T_{max}/dt = 10^7$. Since the system is ergodic and we consider a long trajectory compared to the timescale of the system, the statistics presented here are extremely insensitive to the chosen initial condition. In fact, we have repeated the same procedure for a total of five different chaotic trajectories of duration $T_{max} = 10^5$ and all the numbers reported below oscillate at most 1%, while in most cases, the oscillation is only of order 0.1%.

Let us denote the set of UPOs of the database as $\mathscr{U} = \{U_k\}_{k=1}^{M}$ where the UPO U_k is intended as a set of points in the system phase space $U_k = \{u_k(s)\}_{s=1}^{dt*T_k}$, with T_k being its period. We define a metric of proximity that allows us to select and rank the closest UPOs to the trajectory at each point in time. More precisely, we say that the UPO $U_{\bar{k}}$ has the closest pass to the chaotic trajectory $\mathscr{X}_{chaotic}$ at time t if

$$\min_s |u_{\bar{k}}(s) - x(t)| = \min_k(\min_s |u_k(s) - x(t)|). \tag{5}$$

It is important to notice that closeness and shadowing become equivalent when (5) becomes infinitesimal. The minimal distance between a UPO and the chaotic trajectory decreases as we consider complete sets of UPOs with larger maximum symbolic lengths. The statistics of such a distance for the case studied here is shown in Fig. 3(a) and discussed below. We can then define the *ranked shadowing*, where for each point x_t along the chaotic trajectory $\mathscr{X}_t$ we rank the UPOs according to their distance from x_t. Note that after

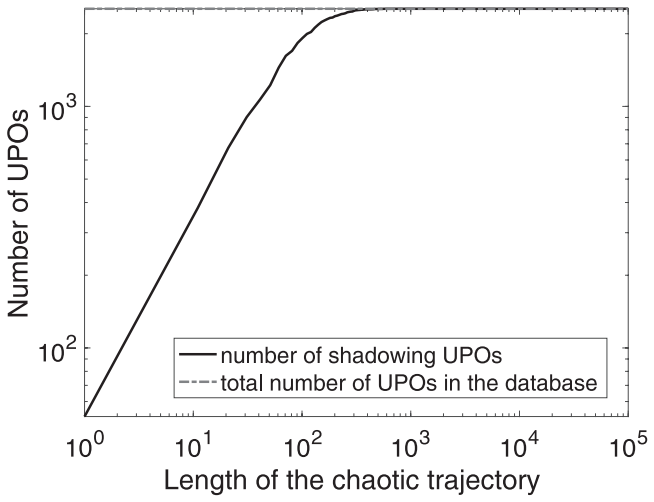

FIG. 2. Number of shadowing UPOs as a function of the length of the shadowed chaotic trajectory.

a time step the distance between a given UPO and the chaotic trajectory will change, while its rank UPO might stay the same or also change. The supporting data[43] includes a hopefully informative video that illustrates how UPOs shadow the chaotic trajectory.

This calculation was carried out using all available periodic orbits (see Appendix A for more details on the algorithm specification). Clearly, it is important to test whether all the UPOs of our database rank shadow at least once the chaotic trajectory.

We can see in fact from Fig. 2 that the number of UPOs $N_U(t)$ that perform rank shadowing at least once grows very rapidly with the length of the trajectory t. We find an approximate power law $N_U(t) \propto t^\alpha$ with $\alpha \approx 0.78$ for moderate values of t up to ≈ 100. A chaotic trajectory having a duration of 10^3 time units already saturates the database so that when considering a trajectory of duration $T_{max} = 10^5$ all UPOs in the dataset shadow the trajectory multiple times.

The reader might think that the definition of shadowing proposed in Eq. (5) could be unreasonably strict. In fact, at each time step, we are only selecting the nearest UPO, thus possibly discarding many other UPOs that are also extremely close to the trajectory. Hence, we also propose a looser definition of shadowing that allows to take into account the fact that a UPO might still be nearby the trajectory even if it is not anymore the nearest one. In particular, if U_t is the closest UPOs to the trajectory at time step t, we say that U_t persists in shadowing at time step $t+1$ if by then U_t is one of the K closest UPOs, or, in other terms, it belongs to one of first K tiers. In this fashion, we are rewarding the quality of the shadowing of the UPOs within the first K tiers. When the UPOs exits the first K tiers of shadowing, the closest UPO to the trajectory is selected as shadowing UPO. In this article, we will consider various values of K ($K = 1$ corresponding to the original, strictest definition of shadowing) in order to assess the robustness of our results.

In general, the shadowing UPOs are characterized by two properties. First, by definition, they have close proximity with the chaotic trajectory. Additionally, since the flow is smooth, we expect a certain degree of persistence in the shadowing: if a UPO is near the chaotic trajectory, the velocity fields will also be similar, and one expects that the UPO will persist its shadowing property for a certain time. The persistence, namely, the mean time duration of the shadowing process, quantifies the temporal co-evolution of the chaotic trajectory with the approximating UPOs. In the present discrete numerical implementation of the ranked shadowing process, it is possible that the closest UPO might not be the orbits that have higher persistence. However, even in the case of the existence of another orbit with higher persistence, the bounds on the velocity field and, more importantly, on the norm of the Jacobian of such field guarantee that the selected orbit, chosen solely based on the proximity criteria, would stay close to the trajectory for a certain period of time. We could quantify this information by noticing that the mean speed over the attractor is about 26 with standard deviation about 9. This results in an average displacement of about 0.26 for the considered numerical discretization $dt = 0.01$.

Figure 3(a) presents the probability distribution functions (pdfs) of the distance of the shadowing UPOs for tiers $K \in \{1, 10, 30, 100\}$. By definition, as we look at successive tiers, the average distance of the shadowing UPOs with the chaotic trajectory increases, going from $\mathcal{O}(10^{-2})$ for $K = 1$ up to $\mathcal{O}(10^{-1})$ for $K = 100$. More precisely, the mean distance is, respectively, 0.0189, 0.0649, 0.1130, and 0.2106 for the orbits in tier 1, 10, 30, and 100. One should keep in mind that tier $K = 100$ includes the top 4% of the UPOs. Note that substantial overlaps exist between the various pdfs, thus indicating that, in absolute terms, the quality of the shadowing varies throughout the attractor. As we could further quantify in Table I, the quality of the shadowing is, in general, very high: even considering the weakest definition of shadowing, only about 2% of the recorded distances are above 1. Choosing the strictest definition of shadowing, only 0.1% of the recorded distances are above 0.1. This can be better appreciated also by considering that the attractor of the L63 model is contained in the Cartesian product $\mathcal{P} = [-20, 20] \times [-27.5, 27, 5] \times [1, 48]$.[60] One can cover this region with $103\,400 \times 10^{3l}$ cubes of equal size 10^{-l}. We will use such a partition (for $l = 0$) later in the paper.

Figure 3(b) shows the distribution of the mean persistence of the shadowing UPOs when we consider the strict as well as looser definitions of shadowing, with $K \in \{1, 10, 30, 100\}$. By construction, the mean persistence increases with K as we are using looser and looser criteria for defining it. Note that in all cases, the time persistence is strictly larger than four time steps, meaning that our procedure captures in all cases at least some co-evolution of the chaotic trajectory and the approximating UPOs. This also suggests that the adopted temporal resolution for our chaotic trajectory and UPOs is sufficient: had we chosen a longer time step, we would have lost the property of co-evolution. Specifically, the mean persistence is 0.0880, 0.2218, 0.3846, and 0.7371 (corresponding to approximately 9, 22, 38, and 74 time steps) when allowing for fluctuations, respectively, in the first and first 10, 30, and 100 tiers. In the latter case, persistence is of the same order as the Lyapunov time (Λ_1^{-1}). These average temporal durations translate into average rectified distances of co-evolution of about 2, 5, 10, and 19.

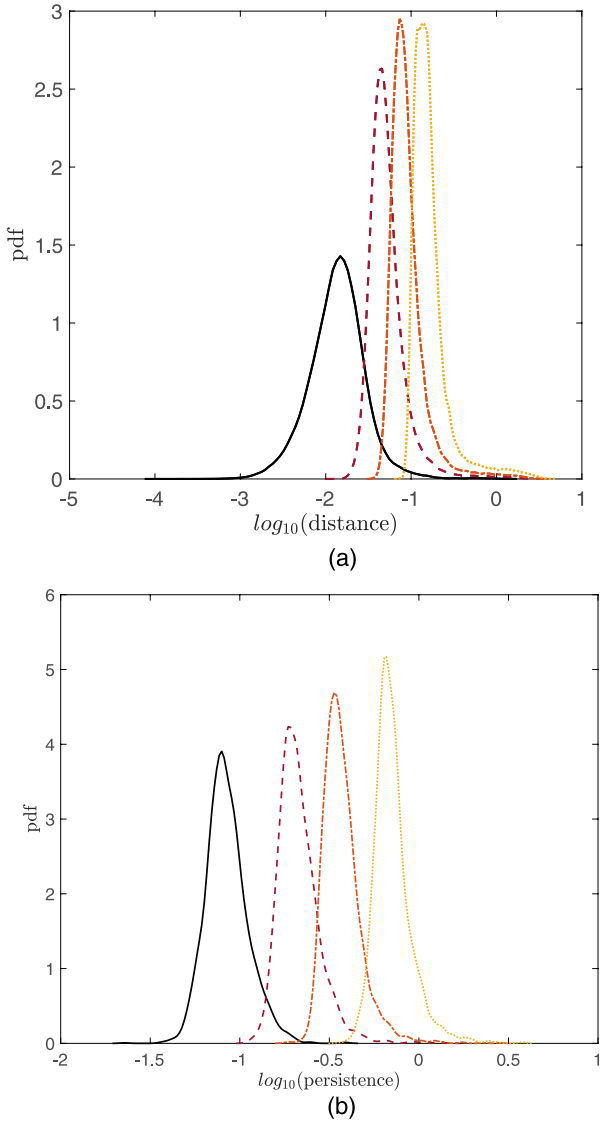

FIG. 3. Panel (a): Probability distribution function for the $\log_{10}$-distance distribution of the first tier orbits (solid black line; mean distance 0.0189), tier $K = 10$ orbits (dashed red line; mean distance 0.0649 dashed red), tier $K = 30$ orbits (dashed and dotted orange line; mean distance 0.1130), and tier $K = 100$ orbits (dotted yellow line; mean distance 0.2106). Panel (b): Probability distribution function of $\log_{10}$-persistence of the tier 1 orbits (solid black line; mean persistence 0.0880) and the shadowing orbits with modified definition allowing for fluctuations within the first $K = 10$ tiers (dashed red line; mean persistence 0.2218), $K = 30$ tiers (dashed and dotted orange line; mean persistence 0.3846), and $K = 100$ tiers (dotted yellow line; mean persistence 0.7371). See the main text for further details.

These figures are larger by a factor $\mathcal{O}(10^2)$ than the corresponding average distances between the chaotic trajectory and the shadowing UPOs, thus reinforcing our claim that the shadowing is accurate and persistent.

TABLE I. Probability that the distance between the chaotic trajectory and the shadowing UPO exceeds the indicated thresholds.

	$P(d > 1)$	$P(d > 10^{-1})$	$P(d > 10^{-2})$
Tier 1	0.0001	0.0096	0.6891
Tier 10	0.0026	0.0816	1
Tier 30	0.0076	0.2997	1
Tier 100	0.0230	0.9551	1

E. Longer period UPOs shadow the trajectory for a longer time

We define the *shadowing time* of a UPO as the total amount of time that the UPO spends shadowing the chaotic trajectory. More precisely, if the UPO U_k is selected as shadowing orbit t_k times, its shadowing time will be $\tau_k = t_k * dt$. This quantity is a good indicator for the absolute shadowing time but it does not take into account the length of the UPO. Longer period UPOs correspond to a longer trajectory in phase space. We then introduce the *occupancy ratio* for the UPO U_k, defined as $o_k = \frac{t_k}{T_k/dt}$ with T_k being the period of the UPO. In this way, we are able to measure the shadowing time normalized over the period of the UPO. An occupancy ratio much larger than one indicates that it is likely that a large portion of the UPO has shadowed the trajectory at least once.

One could interpret the trace formula given in Eq. (3) as suggesting that on the average low period orbits should dominate in terms of shadowing a chaotic trajectory because the statistical weight of long period orbits is exponentially suppressed. Instead, as shown in Fig. 4, the shadowing time increases with the period of the UPOs, while the occupancy ratio remains the same. This means that, by and large, all the UPOs are selected to shadow the chaotic trajectory with the same weighting, independently of their period. However, since the number of periodic orbits grows exponentially with the period (see Fig. 1) longer orbits overall dominate, as shown in Fig. 5.

In order to assess the robustness of our results, we have studied the shadowing orbits in the first K tiers, with the goal of testing whether even allowing for a looser definition of shadowing UPOs, the role of longer orbits remains consistently dominant. In this context, we are interested in average quantities over all tiers. In particular, we define the *average occupancy ratio* at time t as

$$\bar{o}_t = \frac{1}{K}\sum_{k=1}^{K} o_k, \tag{6}$$

where o_k is the occupancy ratio of the UPO that shadows the trajectory at time t in tier k. Similarly, we define the *average period* and *average shadowing time* at time t. As mentioned above, a given UPO might appear in different tiers at different times.

The robustness of the analysis is confirmed when reproducing the statistics presented in Fig. 4 with K shadowing UPOs. Allowing for more shadowing UPOs does not affect the correlation found in Sec. II when considering average quantities. Note that the numbers reported in Figs. 4(a) and 4(b) scale proportionally to T_{max}.

These findings, which seem at odds with what the trace formula seems to indicate, support the idea that long-period orbits play an important role in computing ensemble averages.[22–24]

III. TRANSITIONS

In this section, we use UPOs as a tool to investigate the mixing properties of the system. The *ranked shadowing* will be used to define the Markov process that describes the sequence of transitions between neighborhoods of UPOs that define the time evolution of the chaotic trajectory.

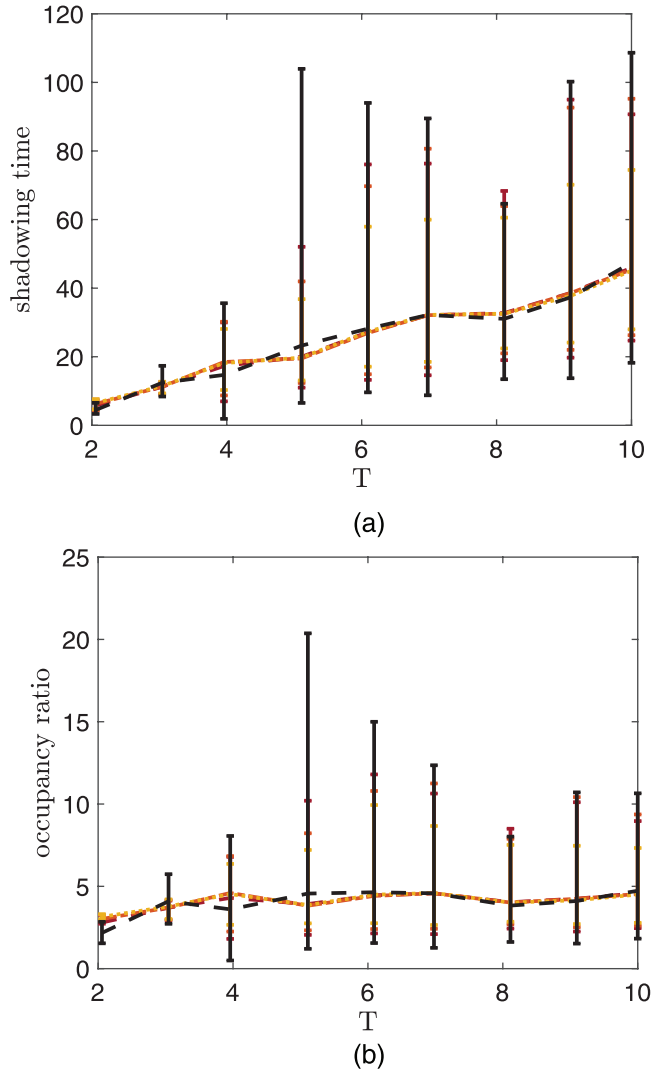

FIG. 4. Average shadowing time [panel (a)] and occupancy ratio [panel (b)] of the first tier (dashed black line) and averaged over first 10 (dashed red), 30 (dashed and dotted orange line), and 100 (dotted yellow line) tiers for UPOs of period T. The bars indicate the range between the percentiles 2.5 and 97.5 for each value of T.

A. Extracting a Markov chain from the dynamics

A very valuable tool to study transitions and the evolution of measures in dynamical systems is offered by the transfer operator. On the attractor, Ω the *Perron–Frobenius operator* or *transfer operator* $\mathscr{P}_t : L^1(\Omega) \to L^1(\Omega)$ is defined as

$$\mathscr{P}_t\rho(x) = \int_\Omega \rho(y)\delta(x - S^t(y))\, dy = \rho(S^{-t}(x))|det(DS^{-t}(x))|, \quad (7)$$

which evolves probabilities densities ρ under the dynamics of the system; note that D indicates the Jacobian. From the study of its spectral properties, we can deduce significant statistical information about the system, such as mixing properties, invariant densities, and decay of correlations.[61,62] For instance, fixed points of $\mathscr{P}_t$ represent invariant densities for the dynamics, which remain unaltered by the flow.

We need to define an appropriate numerical estimate of the transfer operator $\mathscr{P}_t$. In fact, in order to tackle the problem from a numerical standpoint, we have to consider the transfer operator within a finite dimensional setting, where the phase space is not interpreted as a continuum, but it is appropriately discretized into a finite collection of regions, with mass moving from one region to the other at each iteration of the transfer operator. It is important to notice that at this stage, the dynamics occurring within each set of the partition is ignored, and we are just interested in the macroscopic movement of mass. Different methods for defining this approximation have been developed. For the well-known Ulam's method,[40] the approximation takes the form of a regular lattice covering the phase space. See Refs. 62 and 63 for classical results on the use of Ulam's method for approximating the properties of chaotic dynamical systems and[64,65] for recent applications on the L63 model.

We propose here a different way to discretize the dynamics of the system. Similarly to what done in Ref. 41, we select M numerical UPOs $U_1, \ldots, U_M$ and we associate the states $A_1, \ldots, A_M$ obtained

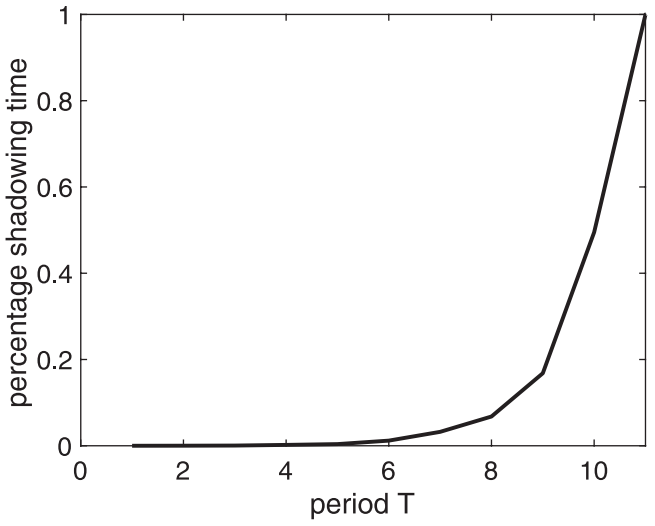

FIG. 5. Cumulative fraction of the shadowing time performed by UPOs having a larger period.

by considering the UPOs together with their neighborhoods. Each A_i represents one of the possible discrete states of the system. We implement the shadowing algorithm: at each time step t, the UPO U_k that minimizes the distance with the chaotic trajectory is selected (see Sec. II D for more details on the algorithm). Hence, we say that the system is in the state A_k at time t. The stochastic variable $s : \{1, \ldots, N_{max}\} \subset \mathbb{N} \to \mathscr{A}$ describes the shadowing process just outlined as follows:

$$s(t) = A_k, \tag{8}$$

with A_k being the shadowing UPO at time t and corresponding neighborhood. We then construct the stochastic matrix as

$$P^{dt}_{i,j} \approx \frac{\#\{k : (s(k) = A_j) \wedge (s(k+1) = A_i)\}}{N_{chaotic}}, \tag{9}$$

where # defines the cardinality of the set.

B. Spectral properties of the transfer operator

In this section, we use the spectrum of the stochastic matrix P^{dt} to study the mixing properties of the system. We focus on the process of scattering that the forward trajectory undergoes by being repelled continuously between the neighborhood of the various UPOs.

Let us recall a few basic properties of the spectrum of a general stochastic matrix. Its leading eigenvalue is $\lambda = 1$, and its corresponding eigenvector $\mathbf{w}^{(1)}$, in the case of an ergodic Markov chain, determines the unique invariant measure. The other eigenvalues, which can be proven to be inside the unit circle, fulfill the condition $\sum_j w^{(\lambda)}_j = 0$, where $w^{(\lambda)}_j$ indicates the j^{th} component of the eigenvector $w^{(\lambda)}$. The subdominant eigenvalues, ordered accordingly to $1 > \Re(\lambda_2) \geq \Re(\lambda_3) \geq \cdots \geq \Re(\lambda_M)$ (where $\Re$ indicates the real part), can be thought of as modes of decay, as they determine the time scale of convergence to the stationary probability measure. We can quantify these time scales by defining the corresponding decay rate as $\tau_k = -\frac{dt}{log(\Re(\lambda_k))}$, where dt takes into account how we have discretized the dynamics in the time domain. In particular, τ_2 identifies the mixing time scale.[44]

We derive the matrix P^{dt} following the procedure outlined in Sec. III A, by considering the shadowing of a chaotic trajectory with length $T_{max} = 10^5$ with the full set of $M = 2536$ UPOs. P^{dt} is a stochastic matrix by construction, its first eigenvalues are $\lambda_1 = 1, \lambda_2 = 0.9841, \lambda_3 = 0.9806$, and $\lambda_4 = 0.9706$ and the corresponding decay rates are $\tau_2 = 0.6239, \tau_3 = 0.5104$, and $\tau_4 = 0.3351$. We also verified that there exists a value $\hat{N}$ so that $P^{\hat{N}}_{i,j} \neq 0 \; \forall \; i, j$, implying that the process is ergodic. Additionally, we tested the Markovianity of the process by verifying that the stochastic matrix P^{ndt} defining the scattering sampled every $n > 1$ time steps of the chaotic trajectory between the neighborhoods of the various UPOs has very similar dominant eigenvectors as those of P^{dt}, while the corresponding eigenvalues scale, with a good approximation, with the n^{th} power, as expected.

C. Quasi-invariant sets

We wish to attempt an interpretation of the eigenvectors of P^{dt} corresponding to the subdominant eigenvalues. Let $\mathbf{w}^{(k)}$ be the eigenvector associated with λ_k, $k \geq 2$. This allows us to define two sets B_1 and B_2,

$$B_1 = \bigcup_{i \in \mathscr{I}_1} A_i \quad where \quad \mathscr{I}_1 = \{i : \varsigma(w^{(k)}_i) = 1\}, \tag{10}$$

$$B_2 = \bigcup_{i \in \mathscr{I}_2} A_i \quad where \quad \mathscr{I}_2 = \{i : \varsigma(w^{(k)}_i) = -1\}, \tag{11}$$

where $\varsigma(w^{(k)}_i) = \text{sign}(w^{(k)}_i)$. The sets B_1 and B_2 corresponding to the eigenvectors $w^{(k)}, k = 2, 3, 4$ are presented in Fig. 6. We propose that regions characterized by the same color (red and blue in our figures) are associated with separate bundles of UPOs. As we will see below, for each eigenvector, the red (blue) regions describe parts of the attractors with positive (negative) anomalies of the density with respect to the invariant one. The forward trajectory undergoes transitions between the neighborhood of the UPOs belonging to a bundle and is repelled with low probability toward the neighborhood of a UPO belongs to the other bundle. The closer to one the real part of an eigenvalue is, the less efficient is the exchange between regions of different colors in the corresponding mode. More precisely, the subdominant eigenvectors $w^{(k)}$ provide an ordering of the quasi-invariant structures in terms of "leakiness."

Keeping in mind that each individual UPO is an actual invariant set and provides an exact solution of the evolution equations, we propose that our method defines structures that are closely related to the so-called quasi-invariant sets.[42,66–69] Loosely speaking, quasi-invariant sets are macroscopic dynamical structures such that the probability of individual trajectories beginning in the subset would leave it in a short time is very little (see Appendix B for more details). In particular, the red and blue regions in Figs. 6(a)–6(c) closely resemble the structures defined by the first three Fiedler vectors defining the connectivity of the graph describing the mass transport of the L63 model [Figs. 5(a), 5(b), and 6 in Ref. 62].

D. Relaxation modes

The red-and-blue representation of the subdominant modes given in Figs. 6(a)–6(c) is essentially qualitative because we distinguish the various UPOs only in terms of the sign of their projection on the eigenvectors. We want now to portray the eigenmodes in $\mathbb{R}^3$ in such a way that it is possible to retain quantitative information associated with the evolution of ensembles of trajectories. We proceed as follows. We partition the compact subset of $\mathbb{R}^3$ given by the Cartesian product $\mathscr{P} = [-20, 20] \times [-27.5, 27, 5] \times [1, 48]$. As mentioned before, this set includes the attractor of the L63 model. We cover this region with 103 400 cubes $\mathscr{D} = \{D_i\}_{i=1}^{103\,400}$ with sides having a unitary length. The cubes are built having adjacent sides so that $\mathscr{D}$ constitutes a partition of $\mathscr{P}$. Each UPO and corresponding neighborhood intersects a certain number of cubes and each cube might contain contributions from different orbits. We now define a quantity (mass) that weights the contribution given by UPOs of different types within each cube. We set a fixed number of points $\bar{N}$ to be represented in the phase space *a priori* and assign the points to the different UPOs and relative neighborhood depending on the weight given by the corresponding component of the eigenvector $w^{(k)}$. These points are chosen along the orbits equally spaced in time.

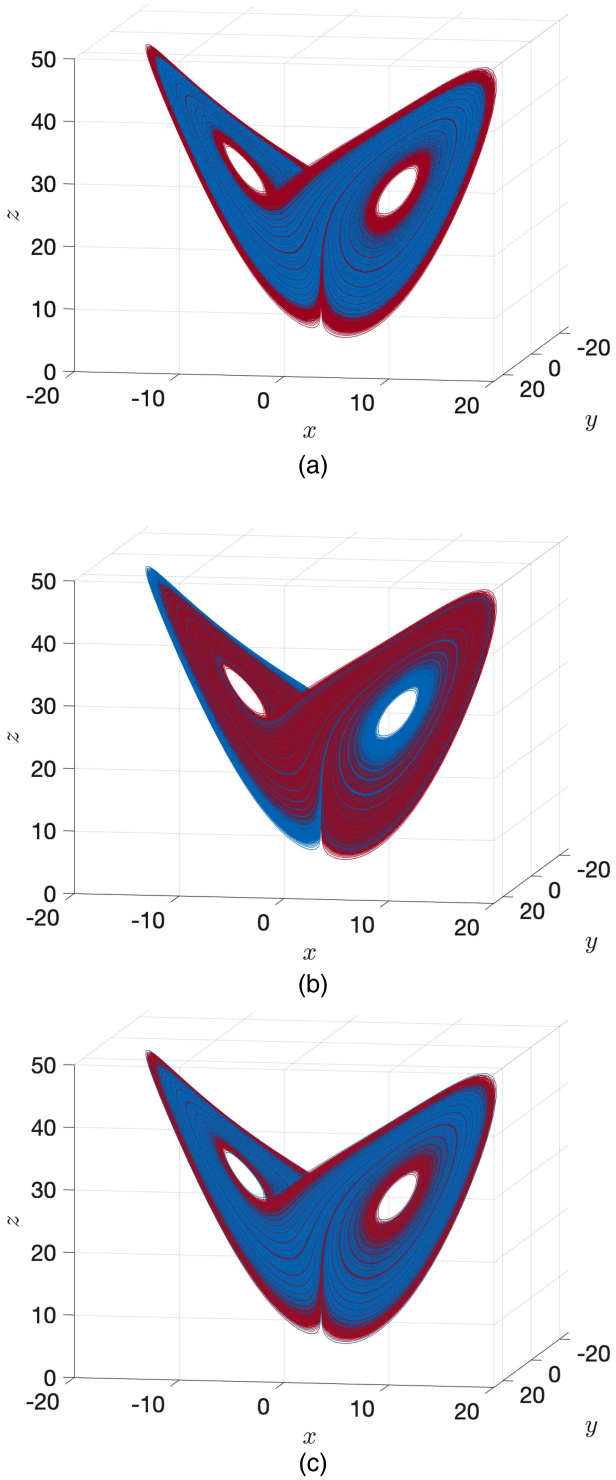

FIG. 6. Quasi-invariant bundles of UPOs obtained with the method outlined in Sec. III C. (a) $\lambda_2 = 0.9841$, $\tau_2 = 0.6239$; (b) $\lambda_3 = 0.9806$, $\tau_3 = 0.5104$; and (c) $\lambda_4 = 0.9706$, $\tau_4 = 0.3351$.

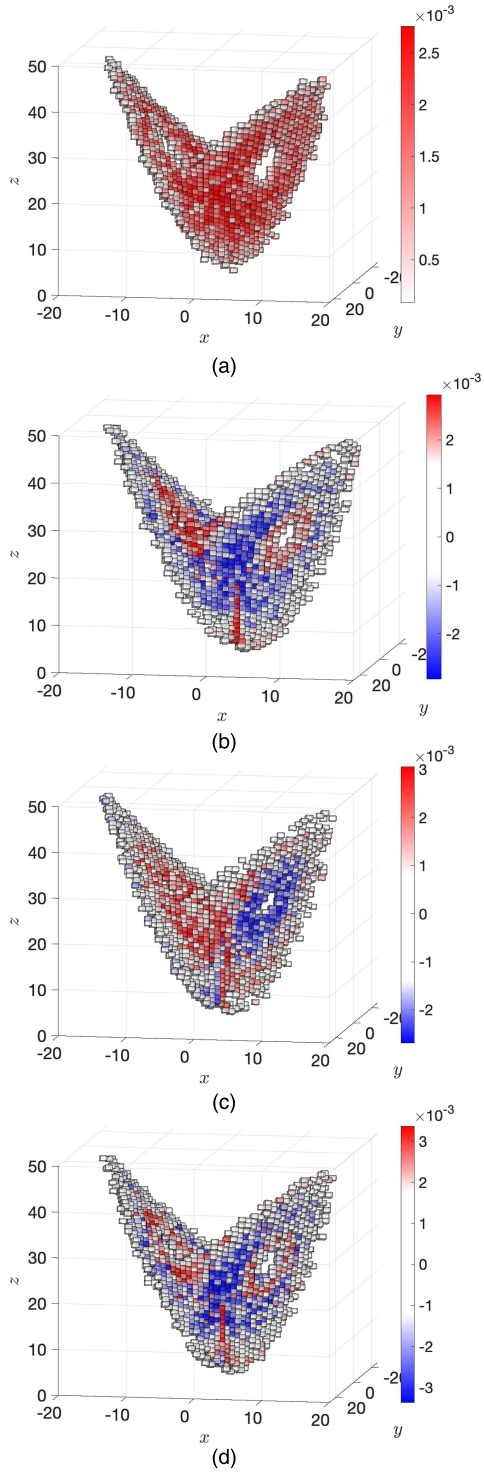

FIG. 7. Invariant measure of the system obtained by projection of $w^{(1)}$ (a). Projection in the phase space of (b) $w^{(2)}$ ($\lambda_2 = 0.9841$), (c) $w^{(3)}$ ($\lambda_3 = 0.9806$), and (d) $w^{(4)}$ ($\lambda_4 = 0.9706$).

We also distinguish between negative and positive contributions, depending on the sign of the component $w_i^{(k)}$. We finally quantify the mass contained in each cube D_i of the partition by calculating the algebraic sum of the points contained in it.

Correspondingly, Fig. 7(a) describes the invariant measure, while Figs. 7(b)–7(d) describe the eigenvectors corresponding to the subdominant eigenvalues λ_2, λ_3, and λ_4, respectively. The eigenvectors $w^{(2)}$, $w^{(3)}$, and $w^{(4)}$ are the three slowest modes responsible for the relaxation of an initial probability measure toward the invariant one, the rate of convergence being given by the corresponding eigenvalues. By construction, one can see a good correspondence between the red and blue regions in the panels of Figs. 6 and 7 associated with the same eigenvalue. Indeed, the physical process responsible for the slow decay of anomalies of an ensemble with respect to the invariant measure described in Fig. 7 is indeed the slow mixing occurring in phase space between the regions described by the quasi-invariant sets associated with different bundles of UPOs depicted in Fig. 6. We observe that the smaller the eigenvalue, thus associated with faster decay rate, the finer the geometrical structure associated with the mode. This agrees with our intuition on how diffusion works.

E. Remark

The reader might wonder how robust the results presented in Figs. 6(a)–6(c) and Figs. 7(a)–7(d) with respect to the shadowing criteria defined in Eq. (5), which takes into consideration only tier 1 shadowing UPOs. To assess the robustness of the method, we have repeated our analysis using the looser definition of shadowing described in Sec. II D, which leads to increased persistence of the co-evolution of the chaotic trajectory and the shadowing UPOs described in Fig. 3(b). The results are presented in the supporting data.[43] The subdominant eigenvectors change very little as larger values of K are considered, whereas, as expected, the value of the corresponding eigenvalues gets closer and closer to 1 so that slower decay of correlation is found. Clearly, this is the probabilistic counterpart of the results shown in Fig. 3(b) and supports the idea expected since allowing for more persistence in the shadowing of the chaotic trajectory results in less frequent transitions and thus slower decay rates.

IV. SUMMARY AND CONCLUSION

The theory of UPOs has found extensive applications in the study of low-dimensional chaotic systems, in particular, as a means to calculate dynamical averages through the use of trace formulas.[17,49,50] In recent times, promising developments have been made regarding its use for understanding the behavior of higher dimension dynamical systems.[25,30–33,35] Very recently, efforts have been dedicated to better understanding the similarity of chaotic trajectory segments and locally approximating UPOs in fluid flows.[38,39] It is usually assumed that the low-period UPOs are the most relevant ones for achieving an accurate representation of the statistical properties of the system.[17–21] Nonetheless, even if the trace formulas[8] seem to suggest the opposite, it is sometimes found that long-period UPOs can be of great importance for computing statistical averages.[22–24] Additionally, UPOs have been used as a way to perform coarse-graining: it has been shown that it is possible to approximate accurately the evolution of a fluid flow using a finite-state Markov chain where each state corresponds to the neighborhood of UPOs.[41] Finally, specific UPOs have been shown to be key to separating quasi-invariant sets for the L63 model.[70]

In this work, we have attempted to bring together these research lines by performing an accurate analysis of how a long chaotic trajectory of the L63 model with the standard parameter values can be approximated using the complete set of UPOs having symbolic dynamics with a period up to 14, numbering 2536 UPOs. The chaotic trajectory can be seen as a continuous process of scattering between the neighborhood of the various UPOs. At each time step, we rank the UPOs in terms of their distance to reference point and investigate how the distances and the ranking changes in time. The shadowing of the trajectory involves both proximity and the fact that, as a result of the smoothness of the flow, the reference point of the trajectory and the considered UPOs co-evolve; indeed, the rectified distance of the co-evolving UPO with the trajectory is orders of magnitude larger than the initial distance between the two. We find that longer UPOs, as a result of their higher number and longer spatial extent, are the most effective in shadowing the orbit of the system. This holds true if we consider a relaxed version of our algorithm, which allows for the rank of the shadowing UPO to fluctuate up to a certain threshold (*very good* vs *optimal* shadowing).

We then investigated a finite-state representation of the dynamics where each state is given by an UPO and its neighborhood, and the stochastic matrix is defined in a frequentist way by studying the transitions defining the time-dependent shadowing of the chaotic trajectory. Since we are implementing a discretized representation of the transfer operator, the eigenvectors corresponding to the subdominant eigenvalues describe the process of relaxation of ensembles toward the invariant measure. While a similar UPOs-based Markov chain model has been recently proposed by Ref. 41 with the goal of computing averages, to the best of our knowledge, this is the first time this specific discretization is performed with the purpose of analyzing the mixing properties of the system. By projecting the UPOs on the 3D space, we find that eigenvectors with finer spatial structures have faster decaying rates. Additionally, building on the fact that UPOs are invariant sets that transport mass across the attractor, the regions of the eigenvectors having the same sign can be thought as approximately defining quasi-invariant sets. Indeed, the patterns defined in this way exhibit qualitative agreement with the structures found in the L63 model by Froyland *et al.* in Refs. 62 and 70 using the discretization of the transfer operator based on the classical Ulam's partition. We interpret our findings as follows. The forward trajectory typically undergoes scattering between UPOs belonging to a bundle of UPOs associated with a quasi-invariant set, while, rarely, the scattering process brings the trajectory to the proximity of a UPO belonging to the other bundle, associated with a competing quasi-invariant set.

Clearly, further research is needed in this direction in order to assess the differences and similarities between these approaches. Our procedure seems to have a good degree of robustness. It is encouraging to see that if we construct the stochastic matrix using the relaxed definition of the shadowing mentioned above, the eigenvectors corresponding to the subdominant eigenvalues are virtually unchanged, whereas the decay rates become slower, as

persistence is enhanced by slowing down the transitions between the competing neighborhoods.

This work provides further support to the potential of using UPOs for reaching a comprehensive understanding of the properties—averages and correlations—of chaotic dynamical systems. We would like to extend this analysis to a higher dimensional system of practical relevance. In particular, we would like to extend the work of Lucarini and Gritsun[35] on blocking events, investigating transitions between zonal flow and blocking by applying the methodology developed in this paper. The investigation of this model is of interest both in terms of the physical process of interest—the low-frequency variability of the atmosphere is far from being a settled problem—and in terms of its mathematical properties, as it is characterized by high variability in the number of unstable dimension, thus featuring a serious violation of hyperbolicity.

ACKNOWLEDGMENTS

The authors have benefitted from scientific exchanges with P. Cvitanović, J. Dorrington, G. Ducci, G. Froyland, C. Nesbitt, M. Santos, N. Zagli, and M. Zaks, and from the very constructive criticism by two anonymous reviewers. A.G. was supported by the Moscow Center of Fundamental and Applied Mathematics (Agreement No. 075-15-2019-1624 with the Ministry of Education and Science of the Russian Federation). V.L. acknowledges support received from the EPSRC (Project No. EP/T018178/1) and from the EU Horizon 2020 project TiPES (Grant No. 820970). C.C.M. has been supported by an EPSRC studentship as part of the Centre for Doctoral Training in Mathematics of Planet Earth (Grant No. EP/L016613/1). The authors acknowledge support received from the Institutional Sponsorship–International Partnerships–University of Reading (Grant No. EP/W524268/1).

AUTHOR DECLARATIONS

Conflict of Interest

The authors have no conflicts of interest.

DATA AVAILABILITY

The data that support the findings of this study, extra figures, videos, and further details on the methodology can be accessed through the project "Decomposing the Dynamics of the Lorenz 1963 model using Unstable Periodic Orbits: Averages, Transitions, and Quasi-Invariant Sets" and are openly available in Figshare at https://tinyurl.com/njs6dupe Ref. 43.

APPENDIX A: UNSTABLE PERIODIC ORBITS SEARCH

We will review here the classic Newton algorithm[71] for detecting UPOs of the ordinary differential equation

$$\dot{x} = f(x), \quad x \in \mathcal{M}, \tag{A1}$$

where $\mathcal{M} \subset \mathbb{R}^n$ is a compact manifold. This method is particularly appropriate for finding periodic solutions even in high-dimensional systems.

The problem of numerically finding UPOs can be reduced to the solution of the periodicity condition, which corresponds to a system of nonlinear equations with respect to the initial condition of the UPO and its period,

$$S^T(x_{in}) = x_{in}, \tag{A2}$$

where x_{in} is the initial condition and T is the period of the UPO. Even for simple nonlinear systems, this represents a difficult numerical problem. Hence, the choice of the algorithm and initial guess represent an important aspect to be considered. We first rewrite the periodicity condition (A2) as follows:

$$S^T(x_{in}) - x_{in} = 0. \tag{A3}$$

This is a system of n nonlinear equations (n is the dimension of the phase space) in $n+1$ unknowns (the vector x_{in} and the orbit period T). We start with an initial condition (x_0, T). A way to choose it is by calculating a long trajectory and selecting a quasi-recurrence occurring over a period T such that $|S^T(x_{in}) - x_{in}| < \varepsilon$ with ε decided *a priori*. Let then x^i and T^i be the ith approximations for initial condition and period. The aim of the algorithm is to calculate a correction $(\Delta x_i, \Delta T_i)$ so that we can improve the initial guess in such a way that

$$||S^{T^i+\Delta T_i}(x^i + \Delta x_i) - (x^i + \Delta x_i)|| < ||^{T^i}(x^i) - x^i||. \tag{A4}$$

We obtain the approximate corrections $(\Delta x_i, \Delta T_i)$ by expanding

$$S^{T_{i+1}}(x^{i+1}) - x_{i+1} = S^{T_i+\Delta T_i}(x^i + \Delta x_i) - (x^i + \Delta x_i) = 0 \tag{A5}$$

into a Taylor series with respect to Δx_i and ΔT_i

$$\begin{aligned} &S^{T^i+\Delta T_i}(x^i + \Delta x_i) - (x^i + \Delta x_i) \\ &\approx S^{T^i}(x^i) - x^i + \left(\frac{\partial S^{T^i}(y)}{\partial y}\Big|_{y=x^i} - I \right) \Delta x_i + \frac{\partial S^T(x^i)}{\partial T}\Big|_{T=T^i} \Delta T_i = 0, \end{aligned} \tag{A6}$$

where I is the identity matrix of order n. $\frac{\partial S^{T_i}(y)}{\partial y}$ is the tangent linear operator and it is an approximation M_i of the monodromy matrix M.[3] $\frac{\partial S^T(x_i)}{\partial T}\Big|_{T=T^i}$ is the derivative of the solution with respect to time $\dot{x} = f(x)$ evaluated at the final condition $f(S^{T_i}(x_i))$. In order to remove the excess in degrees of freedom, we impose the *phase condition* by requiring the orthogonality of the correction vector to the orbit

$$(f(S^{T_i}(x_i))) \cdot \Delta x_i = 0. \tag{A7}$$

In this way, we reduce the problem of finding the corrections at step i to the solution of a linear system of $n+1$ equations in $n+1$ unknowns

$$\begin{pmatrix} M_i - I & f(S^{T_i}(x_i)) \\ (f(S^{T_i}(x_i)))^T & 0 \end{pmatrix} \begin{pmatrix} \Delta x_i \\ \Delta T_i \end{pmatrix} = \begin{pmatrix} x_i - S^{T_i}(x_i) \\ 0 \end{pmatrix}. \tag{A8}$$

The solution of Eq. (A8) gives the next approximations for the UPO initial condition and period. In some cases, the Newton method may not give convergence (or the convergence could be very slow) if the initial guess is far from the solution so that the linear Taylor expansion is not valid or the linear system is degenerate. In this case, one can use a nonlinear expansion in Eq. (A6) as well as

step relaxation together with line search procedure (see Ref. 32 for more details).

We consider quasi-recurrent orbits as initial conditions. We integrate the system for a long time T_{max} starting from a random initial state; the result is a numerical trajectory consisting of the set of ordered points $\{x\}_{j=1}^{T_{max}}$. We then calculate the quantity $d_{ij} = |x_j - x_i|\ \forall i, j \in \{1, \dots T_{max}\}$ and take the minimum, obtained at say x_m, x_n. We have a pair of points for which the trajectory starting from x_m passes again near the starting point x_m in time $n - m$. We can then consider the pairs $(x_m, m - n)$ as the initial condition for determining the UPO with the Newton method.

The numerical trajectories have been calculated using the midpoint numerical scheme, with an integration time step of 10^{-3}. We choose an output time step $dt = 0.01$ and consider a UPO to be detected when $err^{in} < \varepsilon$ with $\varepsilon = 10^{-10}$.

APPENDIX B: QUASI-INVARIANT SETS

We introduce here some key ideas regarding the macroscopic structures and large scale dynamics of the system. When the behavior of individual trajectory is hard to predict, as it is the case in chaotic systems, the study of the global evolution of densities represents a powerful tool to gain insight into the dynamics. In fact, even if it is not possible to characterize the evolution of a single initial condition, it often happens that we can group the phase space in sets characterized by predictable behavior. Despite chaotic systems being often transitive, this property can be very weak and it is often the case that the phase space can be decomposed in the macroscopic dynamical structure such that the probability of individual trajectories beginning in the subset would leave it in a short time is very little. Trajectories tend to stay for a very long time in one of those regions before entering another region. We call these subsets quasi-invariant sets. More precisely,[70] let $\mathbf{F} : \Omega \in \mathbb{R}^d :\to \mathbb{R}^d$ be a smooth vector field, generating the dynamical system or flow $\{\Phi^t\}_{t\in\mathbb{R}}$, $\Phi^t : \Omega \to \Omega$ be the flow of the autonomous system μ preserved by Φ. We say that a subset $A \subset \Omega$ is *almost-invariant* over the interval $[0, \tau]$ if

$$\rho_{\mu,\tau} := \frac{\mu(A \cap \Phi_{-\tau}(A))}{\mu(A)} \approx 1. \tag{B1}$$

Quasi-invariant sets can also be regarded as a valuable tool to study transport and mixing properties of the flow,[72] by evolving with minimal dispersion.

REFERENCES

[1] H. Poincaré, *Les Méthodes Nouvelles de la Mécanique Céleste: Méthodes de MM. Newcomb, Glydén, Lindstedt et Bohlin. 1893* (Gauthier-Villars it fils, 1893), Vol. 2.
[2] P. Cvitanović, "Periodic orbits as the skeleton of classical and quantum chaos," Physica D **51**, 138–151 (1991).
[3] P. Cvitanovic, R. Artuso, R. Mainieri, G. Tanner, G. Vattay, N. Whelan, and A. Wirzba, *Chaos: Classical and Quantum* (Niels Bohr Institute, Copenhagen, 2005), Vol. 69, p. 25.
[4] C. Grebogi, E. Ott, and J. A. Yorke, "Unstable periodic orbits and the dimensions of multifractal chaotic attractors," Phys. Rev. A **37**, 1711 (1988).
[5] J.-P. Eckmann and D. Ruelle, "Ergodic theory of chaos and strange attractors," Rev. Mod. Phys. **57**, 273–312 (1985).
[6] R. Bowen, "ω-limit sets for axiom a diffeomorphisms," J. Differ. Equ. **18**, 333–339 (1975).
[7] M. C. Gutzwiller, *Chaos in Classical and Quantum Mechanics* (Springer Science & Business Media, 2013), Vol. 1.
[8] P. Cvitanović, "Invariant measurement of strange sets in terms of cycles," Phys. Rev. Lett. **61**, 2729 (1988).
[9] D. Ruelle, *Thermodynamic Formalism: The Mathematical Structure of Equilibrium Statistical Mechanics* (Cambridge University Press, 2004).
[10] D. Ruelle, "Smooth dynamics and new theoretical ideas in nonequilibrium statistical mechanics," J. Stat. Phys. **95**, 393–468 (1999).
[11] A. Katok and B. Hasselblatt, *Introduction to the Modern Theory of Dynamical Systems* (Cambridge University Press, 1997), Vol. 54.
[12] S. Smale *et al.*, "Differentiable dynamical systems," Bull. Am. Math. Soc. **73**, 747–817 (1967).
[13] R. Bowen, "Periodic orbits for hyperbolic flows," Am. J. Math. **94**, 1–30 (1972).
[14] G. Gallavotti, *Nonequilibrium and Irreversibility* (Springer, 2014).
[15] G. Gallavotti, "Chaotic dynamics, fluctuations, nonequilibrium ensembles," Chaos **8**, 384–392 (1998).
[16] G. Gallavotti and E. G. D. Cohen, "Dynamical ensembles in nonequilibrium statistical mechanics," Phys. Rev. Lett. **74**, 2694 (1995).
[17] B. Eckhardt and G. Ott, "Periodic orbit analysis of the Lorenz attractor," Z. Phys. B: Condens. Matter **93**, 259–266 (1994).
[18] P. Cvitanović, "Dynamical averaging in terms of periodic orbits," Physica D **83**, 109–123 (1995).
[19] R. Artuso, E. Aurell, and P. Cvitanovic, "Recycling of strange sets: I. Cycle expansions," Nonlinearity **3**, 325 (1990).
[20] B. R. Hunt and E. Ott, "Optimal periodic orbits of chaotic systems," Phys. Rev. Lett. **76**, 2254–2257 (1996).
[21] T.-H. Yang, B. R. Hunt, and E. Ott, "Optimal periodic orbits of continuous time chaotic systems," Phys. Rev. E **62**, 1950–1959 (2000).
[22] S. M. Zoldi and H. S. Greenside, "Comment on 'optimal periodic orbits of chaotic systems'," Phys. Rev. Lett. **80**, 1790 (1998).
[23] D. Lasagna, "Sensitivity analysis of chaotic systems using unstable periodic orbits," SIAM J. Appl. Dyn. Syst. **17**, 547–580 (2018).
[24] D. Lasagna, "Sensitivity of long periodic orbits of chaotic systems," Phys. Rev. E **102**, 052220 (2020).
[25] G. J. Chandler and R. R. Kerswell, "Invariant recurrent solutions embedded in a turbulent two-dimensional Kolmogorov flow," J. Fluid Mech. **722**, 554–595 (2013).
[26] D. Auerbach, P. Cvitanović, J.-P. Eckmann, G. Gunaratne, and I. Procaccia, "Exploring chaotic motion through periodic orbits," Phys. Rev. Lett. **58**, 2387 (1987).
[27] R. Artuso, E. Aurell, and P. Cvitanovic, "Recycling of strange sets: II. Applications," Nonlinearity **3**, 361 (1990).
[28] E. N. Lorenz, "Deterministic nonperiodic flow," J. Atmos. Sci. **20**, 130–141 (1963).
[29] V. Lucarini, "Evidence of dispersion relations for the nonlinear response of the Lorenz 63 system," J. Stat. Phys. **134**, 381–400 (2009).
[30] P. Cvitanović, "Recurrent flows: The clockwork behind turbulence," J. Fluid Mech. **726**, 1–4 (2013).
[31] G. Kawahara and S. Kida, "Periodic motion embedded in plane Couette turbulence: Regeneration cycle and burst," J. Fluid Mech. **449**, 291 (2001).
[32] A. Gritsun, "Unstable periodic trajectories of a barotropic model of the atmosphere," Russ. J. Numer. Anal. Math. Modell. **23**, 345–367 (2008).
[33] A. Gritsun, "Statistical characteristics, circulation regimes and unstable periodic orbits of a barotropic atmospheric model," Philos. Trans. R. Soc. A: Math. Phys. Eng. Sci. **371**, 20120336 (2013).
[34] A. Gritsun and V. Lucarini, "Fluctuations, response, and resonances in a simple atmospheric model," Physica D **349**, 62–76 (2017).
[35] V. Lucarini and A. Gritsun, "A new mathematical framework for atmospheric blocking events," Clim. Dyn. **54**, 575–598 (2020).
[36] D. Faranda, G. Messori, and P. Yiou, "Dynamical proxies of North Atlantic predictability and extremes," Sci. Rep. **7**, 1685 (2017).
[37] Y.-C. Lai, Y. Nagai, and C. Grebogi, "Characterization of the natural measure by unstable periodic orbits in chaotic attractors," Phys. Rev. Lett. **79**, 649–652 (1997).
[38] G. Yalniz and N. B. Budanur, "Inferring symbolic dynamics of chaotic flows from persistence," Chaos **30**, 033109 (2020).

[39]M. C. Krygier, J. L. Pughe-Sanford, and R. O. Grigoriev, "Exact coherent structures and shadowing in turbulent Taylor–Couette flow," J. Fluid Mech. **923**, A7 (2021).
[40]S. M. Ulam, *Problems in Modern Mathematics* (Courier Corporation, 2004).
[41]G. Yalniz, B. Hof, and N. B. Budanur, "Coarse graining the state space of a turbulent flow using periodic orbits," Phys. Rev. Lett. **126**, 244502 (2021).
[42]G. Froyland, "Statistically optimal almost-invariant sets," Physica D **200**, 205–219 (2005).
[43]C. C. Maiocchi, V. Lucarini, and A. Gritsun (2021). "Supplementary material to the article "Decomposing the dynamics of the Lorenz 1963 model using unstable periodic orbits: Averages, transitions, and quasi-invariant sets," Figshare. https://tinyurl.com/njs6dupe.
[44]A. Pikovsky and A. Politi, *Lyapunov Exponents: A Tool to Explore Complex Dynamics* (Cambridge University Press, 2016).
[45]E. Ott, *Chaos in Dynamical Systems* (Cambridge University Press, 2002).
[46]W. Tucker, "The Lorenz attractor exists," C.R. Acad. Sci., Ser. I: Math. **328**, 1197–1202 (1999).
[47]Z. Galias and P. Zgliczyński, "Computer assisted proof of chaos in the Lorenz equations," Physica D **115**, 165–188 (1998).
[48]W. Tucker, "A rigorous ODE solver and Smale's 14th problem," Found. Comput. Math. **2**, 53–117 (2002).
[49]V. Franceschini, C. Giberti, and Z. Zheng, "Characterization of the Lorentz attractor by unstable periodic orbits," Nonlinearity **6**, 251 (1993).
[50]S. M. Zoldi, "Unstable periodic orbit analysis of histograms of chaotic time series," Phys. Rev. Lett. **81**, 3375 (1998).
[51]Y. Saiki and M. Yamada, "Reply to 'Comment on 'time-averaged properties of unstable periodic orbits and chaotic orbits in ordinary differential equation systems'," Phys. Rev. E **81**, 018202 (2010).
[52]Y. Saiki and M. Yamada, "Time-averaged properties of unstable periodic orbits and chaotic orbits in ordinary differential equation systems," Phys. Rev. E **79**, 015201 (2009).
[53]M. A. Zaks and D. S. Goldobin, "Comment on 'Time-averaged properties of unstable periodic orbits and chaotic orbits in ordinary differential equation systems'," Phys. Rev. E **81**, 018201 (2010).
[54]Y. Saiki, "Numerical detection of unstable periodic orbits in continuous-time dynamical systems with chaotic behaviors," Nonlinear Process. Geophys. **14**, 615–620 (2007).
[55]R. Barrio, A. Dena, and W. Tucker, "A database of rigorous and high-precision periodic orbits of the Lorenz model," Comput. Phys. Commun. **194**, 76–83 (2015).
[56]D. Viswanath, "Symbolic dynamics and periodic orbits of the Lorenz attractor," Nonlinearity **16**, 1035 (2003).
[57]Z. Galias and W. Tucker, "Symbolic dynamics based method for rigorous study of the existence of short cycles for chaotic systems," in *2009 IEEE International Symposium on Circuits and Systems* (IEEE, 2009), pp. 1907–1910.
[58]R. Bowen, "Topological entropy and axiom A," in *Proceedings of Symposia in Pure Mathematics* (American Mathematical Society, 1970), Vol. 14, pp. 23–41.
[59]T. Palmer, "Extended-range atmospheric prediction and the Lorenz model," Bull. Am. Meteorol. Soc. **74**, 49–65 (1993).
[60]C. Sparrow, *The Lorenz Equations*, edited by A. V. Holden (Princeton University Press, 1982), p. 111.
[61]V. Baladi, *Positive Transfer Operators and Decay of Correlations* (World Scientific, 2000), Vol. 16.
[62]G. Froyland, "Extracting dynamical behavior via Markov models," in *Nonlinear Dynamics and Statistics* (Springer, 2001), pp. 281–321.
[63]G. Froyland, "Approximating physical invariant measures of mixing dynamical systems in higher dimensions," Nonlinear Anal.: Theory Methods Appl. **32**, 831–860 (1998).
[64]V. Lucarini, "Response operators for Markov processes in a finite state space: Radius of convergence and link to the response theory for axiom a systems," J. Stat. Phys. **162**, 312–333 (2016).
[65]M. Santos Gutiérrez and V. Lucarini, "Response and sensitivity using Markov chains," J. Stat. Phys. **179**, 1572–1593 (2020).
[66]M. Dellnitz and O. Junge, "On the approximation of complicated dynamical behavior," SIAM J. Numer. Anal. **36**, 491–515 (1999).
[67]M. Dellnitz and O. Junge, "Almost invariant sets in Chua's circuit," Int. J. Bifurcation Chaos **7**, 2475–2485 (2011).
[68]G. Froyland, "Unwrapping eigenfunctions to discover the geometry of almost-invariant sets in hyperbolic maps," Physica D **237**, 840–853 (2008).
[69]G. Froyland and M. Dellnitz, "Detecting and locating near-optimal almost-invariant sets and cycles," SIAM J. Sci. Comput. **24**, 1839–1863 (2003).
[70]G. Froyland and K. Padberg, "Almost-invariant sets and invariant manifolds-connecting probabilistic and geometric descriptions of coherent structures in flows," Physica D **238**, 1507–1523 (2009).
[71]T. S. Parker and L. Chua, "Practical numerical algorithms for chaotic systems" (Springer, 1989).
[72]G. Froyland and K. Padberg-Gehle, "Almost-invariant and finite-time coherent sets: Directionality, duration, and diffusion," in *Ergodic Theory, Open Dynamics, and Coherent Structures* (Springer, 2014), pp. 171–216.